Available online at www.sciencedirect.com

SciVerse ScienceDirect

Ceramics International 39 (2013) 347–352

CERAMICS INTERNATIONAL

www.elsevier.com/locate/ceramint

Preparation and characterization of La and Cr co-doped $SrTiO_3$ materials for SOFC anode

Fenyun Yi[a], He Li[a,**], Hongyu Chen[b,c,*], Ruirui Zhao[a], Xiong Jiang[a]

[a]School of Chemistry and Environment, South China Normal University, Guangzhou 510006, China
[b]Base of Production, Education & Research on Energy Storage and Power Battery of Guangdong Higher Education Institutes, Guangzhou 510006, China
[c]Engineering Research Center of Materials and Technology for Electrochemical Energy Storage (Ministry of Education), South China Normal University, Guangzhou 510006, China

Received 11 May 2012; received in revised form 15 May 2012; accepted 11 June 2012
Available online 17 June 2012

Abstract

Using citric acid–nitrate process, La and Cr co-doped A-site deficient $SrTiO_3$ (LSTC) materials were synthesized. The single-phase perovskite structure of LSTC materials can be obtained in airy atmosphere when the dopant content of chromium does not exceed 20 mol%. The LSTC material has excellent chemical compatibility with yttria-stabilized zirconia (YSZ) at 1400 °C. The particle diameters of LSTC powders calcined at 800 °C are all less than 60 nm. The LSTC pellet sintered in air at 1400 °C for 5 h shows a highly densified microstructure composed of polyhedral grains on a micron scale. At 800 °C, the conductivity of LSTC20 pellet is 1.96×10^{-3} S/cm in static air. The conduction activation energy of LSTC20 pellet is calculated to be 0.33 eV in the temperature range of 550–800 °C. The LSTC can be considered as a potential candidate anode material for SOFC with YSZ as electrolyte, but its conductivity needs to be further improved.

Keywords: A. Sol–gel processes; B. X-ray methods; C. Electrical conductivity; D. Perovskites

1. Introduction

Solid oxide fuel cell (SOFC) is the third generation of fuel cells. Besides high efficiency and low pollution, SOFC has various advantages such as all-solid-state structure and fuel flexibility compared with other fuel cells. Therefore, SOFC has been attracting much attention as a power plant and is considered to be the most promising fuel cell [1–3].

At present, the commercialization of SOFC technology is facing three major hurdles which are cost, stability and reliability. The direct utilization of hydrocarbons as the fuels for SOFC is widely perceived as an important step towards reducing the system cost because such a SOFC system allows a much simplified low-cost module design [4].

Despite the fact that the conventional Ni/YSZ cermet anode in SOFC performs brilliantly with hydrogen or syngas as the fuels, it suffers from limitations: (1) the propensity of Ni to catalyze carbon formation when operating the SOFC with hydrocarbon fuels [5,6], (2) the sensitivity to sulfur in fuels [7,8], (3) the sintering of Ni particles and the large Ni–NiO volume change during the redox cycling at SOFC operating temperature, which results in a significant performance degradation [9,10].

Therefore, over the past few years there has been a growing interest in perovskite-based materials in the search for alternative materials to Ni/YSZ cermets as fuel anodes in SOFC [11,12]. The doped strontium titanate is considered as a promising candidate anode material for SOFC in direct hydrocarbon fuels owing to its excellent mixed ionic-electronic conductivity [13,14], electrocatalytic performance for oxidation of hydrocarbon fuels [15–17], ability to be resistant to carbon depositing [18] and sulfur

*Corresponding author at: 378 Outer Ring Road, Guangzhou Higher Education Mega Center, School of Chemistry and Environment, South China Normal University, Guangzhou 510006, China.
Tel./fax: +86 20 39310183.
**Corresponding author. Tel./fax: +86 20 39310187.
E-mail addresses: analchemlh@163.com (H. Li), battery@scnu.edu.cn (H. Chen).

0272-8842/$36.00 © 2012 Elsevier Ltd and Techna Group S.r.l. All rights reserved.
http://dx.doi.org/10.1016/j.ceramint.2012.06.032

poisoning [19,20], and higher structural stability than Ni/YSZ cermet at high temperature [16,21].

In this work, La, Cr co-doped A-site deficient $La_{0.3}Sr_{0.55}Ti_{1-x}Cr_xO_{3-\delta}$ (LSTC) materials were prepared. The phase purity of LSTC materials was analyzed when the dopant content of chromium changes from 10 to 30 mol%. The chemical compatibility between LSTC and YSZ at 1400 °C was investigated. The microstructures of LSTC powders and sintered pellets were observed. The electrochemical impedance spectra of LSTC sintered pellet in static air at different temperatures were measured. In brief, the aim of this work is to research the possibility of LSTC to be used as anode material of SOFC with YSZ as electrolyte.

2. Experimental

2.1. Sample preparation

The LSTC powders were prepared using the following chemical reagents as starting materials: $La(NO_3)_3 \cdot 6H_2O$, $Sr(NO_3)_2$, $Cr(NO_3)_3 \cdot 9H_2O$ and $Ti(OC_4H_9)_4$. Stoichiometric amounts of $La(NO_3)_3 \cdot 6H_2O$, $Sr(NO_3)_2$ and $Cr(NO_3)_3 \cdot 9H_2O$ were dissolved into deionized water to make a nitrate solution, which was marked as solution A. Stoichiometric amount of $Ti(OC_4H_9)_4$ was dissolved into dilute nitric acid solution to make solution B. Solutions A and B were mixed into a uniform mixture. A quantity of citric acid, in a 1.3:1 molar ratio with respect to the total amount of cations, was added into the mixture. The pH value of the resulting solution was adjusted to 7–8 with appropriate quantities of $NH_3 \cdot H_2O$ under continuous stirring at 70 °C and a homogeneous solution was thus formed. With the evaporation of water, a viscous gel of metal–citrate complexes was obtained. The gel was heated up to 200 °C in oven to generate a foam-like black precursor, then it was ground in a mortar and calcined in air between 800 and 1200 °C for 5 h to produce the LSTC powders. When the dopant amount of chromium in LSTC powder is 20 mol%, the powder is labeled as LSTC20. The labeling of the rest is followed by analogy.

The LSTC powders were ground, sieved and pressed uniaxially into pellets at 150 MPa. The green bodies were then sintered in air at 1400 °C for 5 h. After sintering, the color of the pellets changed from pale yellow to black grey. The final pellets were used for SEM observation and electrochemical impedance measurement.

2.2. Sample characterization

Thermal analysis of the conversion of LSTC foam-like precursor to ceramic powder was conducted on a thermogravimetric/differential thermal analysis system (NETZSCH model STA 449C). The black precursor was heated in an open-topped platinum crucible, from room temperature to 1300 °C at a heating rate of 10 °C/min in air. Phase composition of LSTC and LSTC/YSZ powders was identified by X-ray diffraction (XRD) using a Bruker D8 advance diffractometer with Cu-Kα source ($\lambda = 1.54056$ Å) in the Bragg angle range of 20–80°. The microstructures of LSTC powders and sintered pellets were observed using a scanning electron microscope (Carl Zeiss AG—Ultra 55).

Electrochemical impedance spectra of LSTC sintered pellet were obtained using an electrochemical instrument (Autolab PGSTAT302N) in the 0.01–100 KHz frequency range with an excitation voltage amplitude of 10 mV. DAD-87 conductive adhesive was applied onto each face of the sintered pellet and heated afterwards at 800 °C for 0.5 h to obtain a current collection layer. Silver wires were attached to both faces as conductors. The measurements were performed in static air at temperatures from 550 to 800 °C with an interval of 50 °C. Before recording data, the heat preservation time at each temperature was set to 0.5 h so that the sample resistance got stabilized.

3. Results and discussion

3.1. Thermal analysis

Fig. 1 is the simultaneous DSC–TG curves for LSTC20 foam-like precursor. As can be seen from DSC curve, there is a weak endothermic peak at around 92.1 °C, which can be attributed to the volatilization of free water in the foam-like precursor, leading to a mass loss of 4.51% between 60 and 170 °C. The mass loss of 54.28% revealed on the TG curve is likely corresponding to the intensive redox reaction between nitrates and citric acid, which occurs at about 226 °C producing a sharp exothermic peak on the DSC curve. Further mass loss of 19.81% occurred between 350 and 600 °C is suggested to be due to further combustion of the remaining organic groups, accompanied by an exothermic peak at 453 °C on the DSC curve. After these exothermic processes, there are no further major thermal events. The TG curve gradually levels off above 600 °C, and there is only 1.90% mass loss between 600 and 1300 °C, which may be

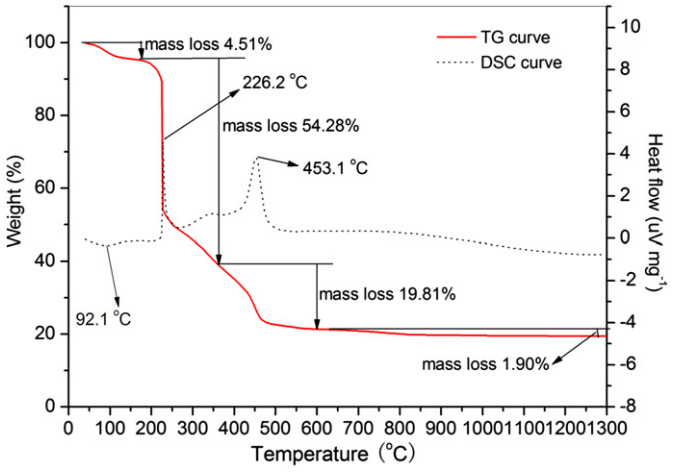

Fig. 1. DSC–TG curves for LSTC20 precursor at a heating rate of 10 °C/min in air.

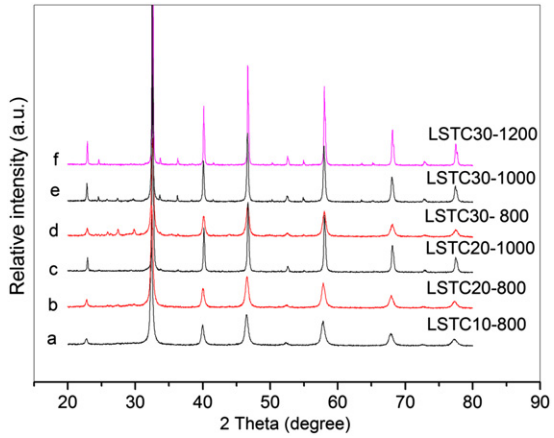

Fig. 2. XRD patterns for LSTC10, LSTC20 and LSTC30 powders.

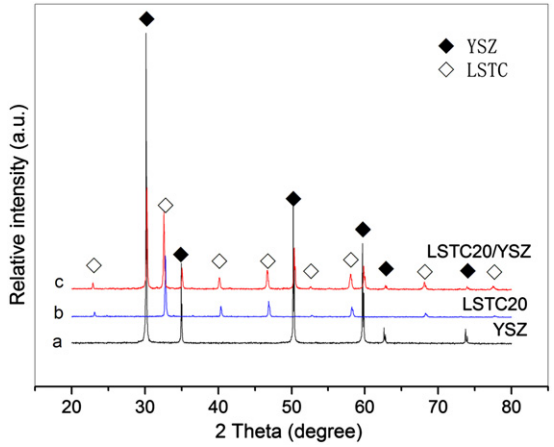

Fig. 3. XRD patterns for YSZ, LSTC20 and LSTC/YSZ sintered at 1400 °C for 5 h.

owing to the detachment of oxygen from crystal lattice. The thermal behavior mentioned above confirms that the majority of the mass loss occurs under 600 °C, which allows for optimization of the heat treatment program.

3.2. Phase characterization

Fig. 2 shows XRD patterns for LSTC10, LSTC20 and LSTC30 powders calcined in air. It can be seen from Fig. 2a that LSTC10 powders calcined in air at 800 °C for 5 h exhibits the formation of a pure phase perovskite structure similar to the standard XRD pattern of undoped $SrTiO_3$ (PDF35-0734). In the XRD patterns for LSTC20 powders, an undesirable $SrCrO_4$ impurity phase is observed at low temperatures and it can be eliminated by heightening the calcination temperature in air from 800 °C up to 1000 °C for 5 h. However, in the XRD patterns for LSTC30 powders, the undesirable $SrCrO_4$ phase still exists when the calcination temperature comes up to 1000 °C for 5 h as shown in Fig. 2e and instead, a new impurity phase of Cr_2O_3 appears. When the calcination temperature increases further to 1200 °C, the $SrCrO_4$ phase disappears and the peak of Cr_2O_3 phase becomes more obvious. It is for this reason that the dopant content of chromium in LSTC cannot exceed 20 mol%.

YSZ is the most widely used electrolyte material in high-temperature SOFC (800–1000 °C). The compatibility between LSTC and YSZ was also investigated by XRD. LSTC20 and YSZ powders were mixed in a mass ratio of 1:1. The mixed powders were ground and pressed uniaxially into pellets at 150 MPa. The green bodies were then sintered in air at 1400 °C for 5 h. The resultant pellets were ground into powder again for measurements. The XRD

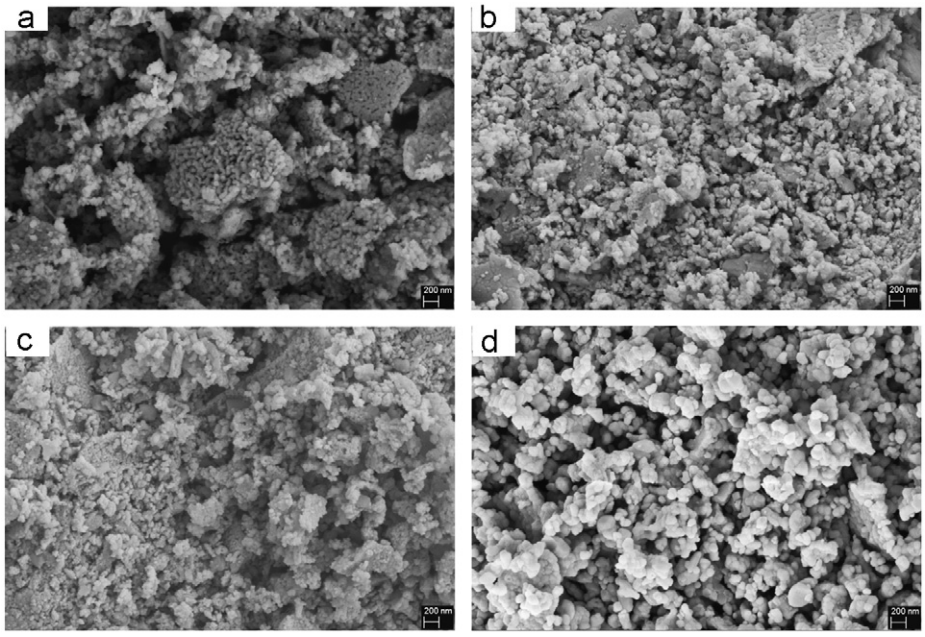

Fig. 4. SEM pictures for LSTC10 powders calcined at 800 °C (a), LSTC20 powders calcined at 800 °C (b), LSTC30 powders calcined at 800 °C (c) and LSTC20 powders calcined at 1000 °C (d).

Fig. 5. SEM picture for the LSTC20 pellet sintered in air at 1400 °C for 5 h.

pattern of the powder is presented in Fig. 3c. From Fig. 3c, it can be seen that there are not any third-phase peaks except the characteristic peaks of YSZ (Fig. 3a) and LSTC20 (Fig. 3b), indicating that no reaction takes place between LSTC and YSZ at 1400 °C. It can thus be concluded that the LSTC material has excellent chemical compatibility with YSZ.

3.3. Microstructure observation

Fig. 4a–c show that the particle diameters of LSTC powders calcined at 800 °C are all less than 60 nm with a small partition of conglomeration, but the effect of the dopant content of chromium seems not significant. However, the effect of temperature on particle diameter is very obvious, and it

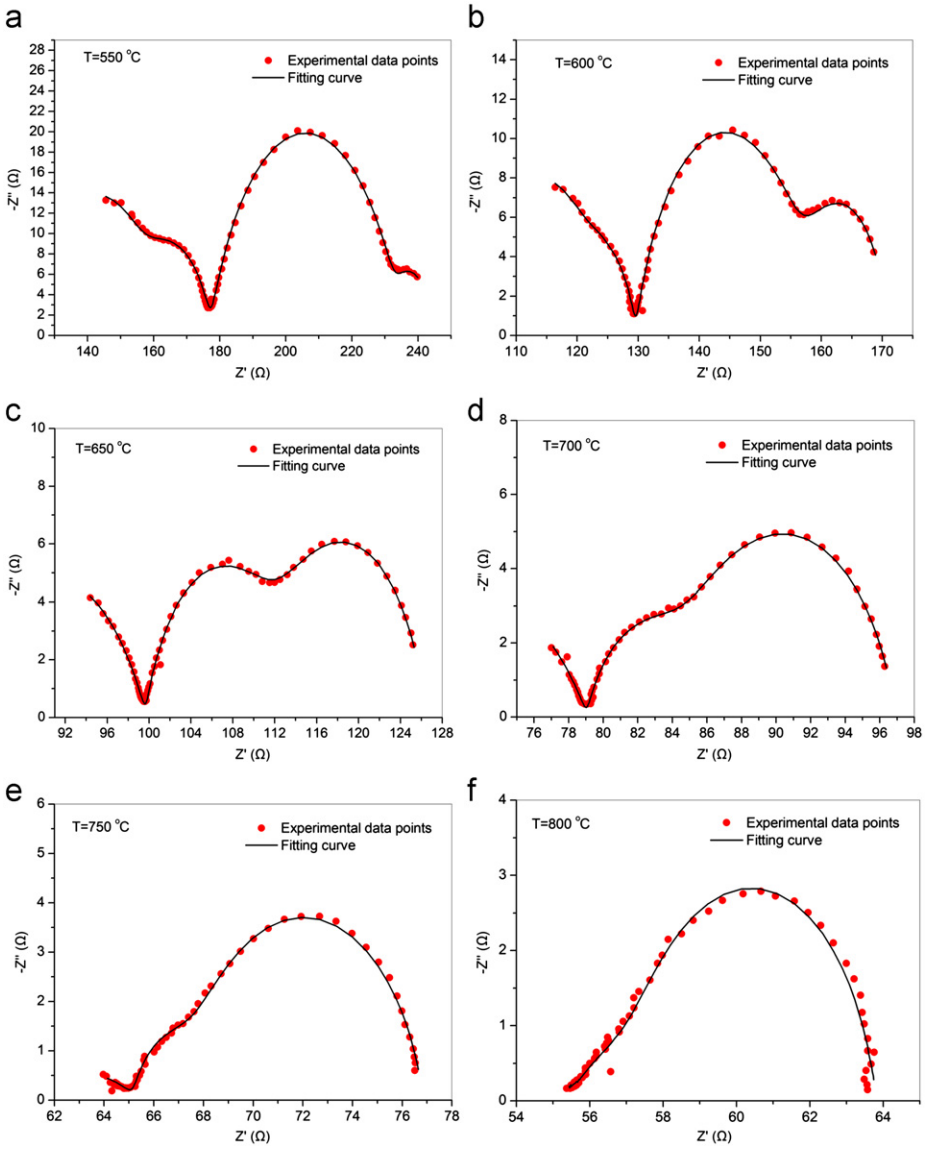

Fig. 6. Nyquist plots for the LSTC20 sintered pellet at various temperatures in static air (a) 550 °C; (b) 600 °C; (c) 650 °C; (d) 700 °C; (e) 750 °C; (f) 800 °C.

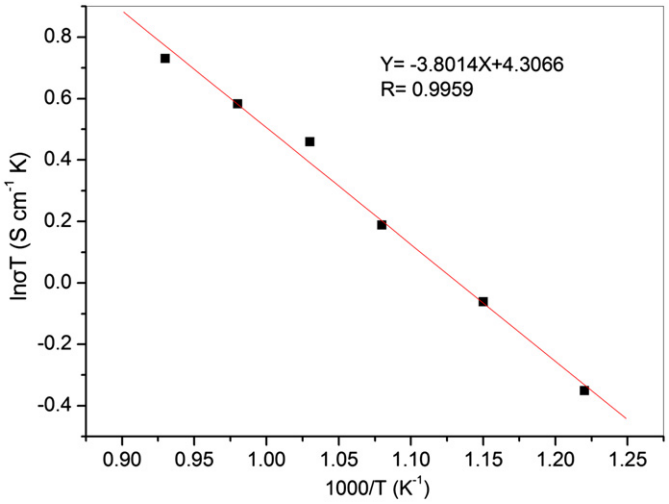

Fig. 7. Arrhenius plot for the LSTC20 sintered pellet in the temperature range of 550–800 °C.

increases with increasing calcination temperature as revealed by the SEM pictures for LSTC20 powders calcined at 800 °C (Fig. 4b) and at 1000 °C (Fig. 4d). The particle of LSTC20 powders calcined at 1000 °C is about 100 nm in diameter. Fig. 4 also indicates that these particles are homogeneous and mostly regularly spherical. This kind of morphology is in favor of die forming and sintering processes.

Fig. 5 is the SEM picture for the LSTC20 pellet sintered in air at 1400 °C for 5 h. It clearly shows a highly densified microstructure composed of polyhedral grains on a micron scale. It is considered that the micron-scale structure is propitious to decrease the electric resistance of grain boundary and increase the conductivity of LSTC sintered pellet. This is vital to the practical processing of LSTC as a SOFC anode component.

3.4. Electrochemical impedance measurement

Electrochemical impedance measurements of the LSTC20 pellet were performed as a function of temperatures in the range of 550–800 °C in static air. Fig. 6 present the typical Nyquist plots obtained at various temperatures. It can be seen from Fig. 6 that the impedance behavior of LSTC20 pellet is rather complicated. There appear four or three overlapped capacitive arcs on the diagram, and both imaginary and real components of the impedance are decreased with increasing temperature. The spectra were fitted using the equivalent circuit $R_s(R_1Q_1)(R_2Q_2)(R_3Q_3)(R_4Q_4)$, or $R_s(R_1Q_1)(R_2Q_2)(R_3Q_3)$, where R_s is the ohmic resistance, the series connection of (R_1Q_1), (R_2Q_2), (R_3Q_3) and (R_4Q_4) corresponds to the four arcs in Fig. 6a and b respectively, and the series connection of (R_1Q_1), (R_2Q_2) and (R_3Q_3) corresponds to the three arcs in Fig. 6c–f respectively. R_i is the resistance and Q_i is the constant-phase element. According to Ohmic resistances (R_s) and the area and thickness of LSTC20 pellet, the conductivities (σ) at various temperatures can be calculated. The result shows that the conductivity increases with increasing temperature. At 800 °C, the conductivity of LSTC20 pellet is 1.96×10^{-3} S/cm in static air. This shows that the conductivity of LSTC materials needs to be improved in further research.

If the Arrhenius equation [22,23] is obeyed in the temperature range of 550–800 °C, the $\ln(\sigma T)$ versus $1/T$ plot for the LSTC20 pellet should be a straight line. That is true of the case as shown in Fig. 7. Thus, the conduction activation energy of the LSTC20 pellet can be found from the slope of the straight line, which is calculated to be 0.33 eV.

4. Conclusions

A doped $SrTiO^3$ material of $La_{0.3}Sr_{0.55}Ti_{1-x}Cr_xO_{3-\delta}$ (LSTC) can be prepared by citric acid–nitrate process, which has a single-phase perovskite structure in airy atmosphere when the dopant content of chromium does not exceed 20 mol%. The LSTC material has excellent chemical compatibility with YSZ at 1400 °C. The particle diameters of LSTC powders calcined at 800 °C are all less than 60 nm. The LSTC pellet sintered in air at 1400 °C for 5 h shows a highly densified microstructure composed of polyhedral grains on a micron scale. At 800 °C, the conductivity of LSTC20 pellet is 1.96×10^{-3} S/cm in static air. The conduction activation energy of LSTC20 pellet is calculated to be 0.33 eV in the temperature range of 550–800 °C. In view of the above performance, LSTC can be considered as a potential candidate anode material for SOFC with YSZ as electrolyte, but its conductivity needs to be further improved.

Acknowledgment

This work was supported by Guangdong Provincial Natural science Foundation of China (S2011040003162 and 10151063101000011).

References

[1] S.C. Singhal, Advances in solid oxide fuel cell technology, Solid State Ionics 135 (2000) 305–313.
[2] K. Joon, Fuel cells—a 21st century power system, Journal of Power Sources 71 (1998) 12–18.
[3] S.P.S. Badwal, K. Foger, Solid oxide electrolyte fuel cell review, Ceramics International 22 (1996) 257–265.
[4] K. Huang, J.B. Goodenough, Solid Oxide Fuel Cell Technology: Principles, Performance and Operations, Woodhead Publishing, Cambridge, 2009.
[5] J.T.S. Irvine, A. Sauvet, Improved oxidation of hydrocarbons with new electrodes in high temperature fuel cells, Fuel Cells 1 (2001) 205–210.
[6] R.J. Gorte, H. Kim, J.M. Vohs, Novel SOFC anodes for the direct electrochemical oxidation of hydrocarbon, Journal of Power Sources 106 (2002) 10–15.
[7] Y. Matsuzaki, I. Yasuda, The poisoning effect of sulfur-containing impurity gas on a SOFC anode: Part I. Dependence on temperature, time, and impurity concentration, Solid State Ionics 132 (2000) 261–269.

[8] Y.X. Lu, S. Laura, A solid oxide fuel cell system fed with hydrogen sulfide and nature gas, Journal of Power Sources 135 (2004) 184–191.
[9] D. Waldbillig, A. Wood, D.G. Ivey, Thermal analysis of the cyclic reduction and oxidation behaviour of SOFC anodes, Solid State Ionics 176 (2005) 847–859.
[10] D. Simwonis, F. Tietz, D. Stover, Nickel coarsening in annealed Ni/8YSZ anode substrates for solid oxide fuel cells, Solid State Ionics 132 (2000) 241–251.
[11] J. Sfeir, $LaCrO_3$-based anodes: stability considerations, Journal of Power Sources 118 (2003) 276–285.
[12] M.J. Escudero, J.T.S. Irvine, L. Daza, Development of anode material based on La-substituted $SrTiO_3$ perovskites doped with manganese and/or gallium for SOFC, Journal of Power Sources 192 (2009) 43–50.
[13] D.P. Fagg, V.V. Kharton, J.R. Frade, A.A.L. Ferreira, Stability and mixed ionic–electronic conductivity of $(Sr,La)(Ti,Fe)O_{3-\delta}$ perovskites, Solid State Ionics 156 (2003) 45–57.
[14] F. Gao, H.L. Zhao, X. Li, et al., Preparation and electrical properties of yttrium-doped strontium titanate with B-site deficiency, Journal of Power Sources 185 (2008) 26–31.
[15] C.Y. Yu, W.Z. Li, W.J. Feng, et al., Oxidative coupling of methane over acceptor-doped $SrTiO_3$, Chinese Journal of Catalysis 13 (1992) 338–344.
[16] O.A. Marina, N.L. Canfield, J.W. Stevenson, Thermal, electrical, and electrocatalytical properties of lanthanum-doped strontium titanate, Solid State Ionics 149 (2002) 21–28.
[17] J. Canales-Vazquez, S.W. Tao, J.T.S. Irvine, Electrical properties in $La_2Sr_4Ti_6O_{19-\delta}$: a potential anode for high temperature fuel cells, Solid State Ionics 159 (2003) 159–165.
[18] J.C. Ruiz-Morales, J. Canales-Vazquez, C. Savaniu, et al., Disruption of extended defects in solid oxide fuel cell anodes for methane oxidation, Nature 439 (2006) 568–571.
[19] R. Mukundan, E.L. Brosha, F.H. Garzon, Sulfur tolerant anodes for SOFCs, Electrochemical and Solid-State Letters 7 (2004) A5–A7.
[20] H. Kurokawa, L. Yang, C.P. Jacobson, L.C. De Jonghe, S.J. Visco, Y-doped $SrTiO_3$ based sulfur tolerant anode for solid oxide fuel cells, Journal of Power Sources 164 (2007) 510–518.
[21] S.Q. Hui, A. Petric, Evaluation of yttrium-doped $SrTiO_3$ as an anode for solid oxide fuel cells, Journal of the European Ceramic Society 22 (2002) 1673–1681.
[22] Y. Li, J.H. Gong, Z.L. Tang, Y.S. Xie, Temperature-independent activation energy for ionic conduction of zirconia based solid electrolytes, Acta Physico-Chimica Sinica 17 (2001) 792–796.
[23] J.A. Kilner, B.C.H. Steele, in: O.T. Sorensen (Ed.), Nonstoichiometric Oxides, Academic Press, New York, 1981, p. 233.